Turkish J. Eng. Env. Sci.
36 (2012) , 139 – 152.

doi:10.3906/muh-1102-9

Effect of horizontal drain size on the stability of an embankment dam in steady and transient seepage conditions

Amir MALEKPOUR[1,*], Davod FARSADIZADEH[1], Ali HOSSEINZADEH DALIR[1]
Jamshid SADREKARIMI[2]
[1] *Water Engineering Department, University of Tabriz, 5166616471, Tabriz-IRAN*
e-mail: Amir_MLK@yahoo.com
[2] *Civil Engineering College, University of Tabriz, Tabriz-IRAN*

Received: 28.02.2011

Abstract

Application of a horizontal drain in an embankment dam has been a prevalent method to lower the phreatic line and dissipate the excessive pore water pressure. The efficiency of this type of drain is often attributed to its length, while the effect of thickness is ignored. In this research, a series of tests were accomplished and different drain sizes including different thicknesses and lengths were applied to a physical model of an embankment dam. During the tests, the pore pressures were measured both in the steady and transient conditions using a number of peizometers and pressure sensors. In steady state, the increased thickness prevented the occurrence of piping and in transient state guaranteed the stability of the upstream slope. However, the thickest drain used in this research showed different efficiencies depending upon the applied length. For the maximum effective length derived from the equations, the increase in thickness could efficiently prevent the undesirable consequences of excessive pore water pressure.

Key Words: Embankment dam, horizontal drain, pore water pressure, factor of safety, transient seepage

1. Introduction

The critical state of steady seepage in an embankment dam occurs when the seepage flow intersects the downstream slope and the piping takes place. According to the comprehensive studies by Foster et al. (2000) and Fell et al. (2003), internal erosion and piping have been the main causes of failure in embankment dams since they destabilize the downstream slope. A well known case of failure due to internal erosion is the Teton Dam in the United States. Mattsson et al. (2008) emphasized that 3 main factors, namely the saturated materials, concentrated seepage, and progressive erosion towards the upstream slope of the embankment dam, accelerate the failure process. Various alternatives have been suggested so far to prevent this problem. In this regard, the application of a horizontal drain has been a common method to control the seepage flow since it can alleviate the pore pressure and lower the phreatic line in the embankment. On the other hand, the transient seepage due to the rapid drawdown of water level in the reservoir is another critical state in an embankment

*Corresponding author

dam that can lead to the failure of the upstream slope. In other words, when the water level declines rapidly within the reservoir the stabilizing effect of hydrostatic pressure on the upstream slope is eliminated, while the pore pressure needs more time to dissipate. Therefore, a high pressure gradient is created in the embankment towards the reservoir and as a result a slip surface may emerge and develop at the upstream slope.

Some famous cases of failure due to rapid drawdown are the Pilarcitos Dam in San Francisco and the Walter Bouldin Dam in Alabama (Berilgen, 2007). There are generally 2 groups of researchers who have worked on the stability of embankment dams in rapid drawdown condition. Lowe and Karafiath (1980), Baker et al. (1993), and the US Army Corps of Engineers (2003) belong to the first group, which assumed the undrained shear strength behavior in the embankment dam. On the other hand, Svano and Nordal (1987), Wright and Duncan (1987), Lane and Griffiths (2000), and Berilgen (2007) are of the second group, which applied the drained shear stress parameters to study the effect of rapid drawdown on the stability of an embankment dam. Drained behavior occurs when the pore water pressure starts to decrease from the outset of the drawdown process and undrained behavior happens when the drawdown is assumed such a quick process that no change in pore water pressure occurs after drawdown. Duncan and Wright (2005) concluded that the time factor of consolidation (T) can determine whether the undrained or drained behavior occurs in the embankment dam. According to their results, more than 99% of the excessive pore pressure is dissipated for $T \geq 3$, which makes the assumption of drained behavior reasonable. Berilgen (2007) highlighted the vital influence of drainage on the stability of embankment dams. According to his studies, presuming the drained behavior for the slow drawdown and the undrained behavior for the fully rapid drawdown, which are 2 limit states, is irrational and the ratio and rate of drainage and the soil permeability are important factors to determine the drainage behavior. For example, he observed undrained behavior for a highly permeable soil in some cases of drawdown in an embankment dam (even for $T \geq 6$). Many studies have been accomplished so far on the design of drain size in steady state seepage (Chahar, 2004; Mishra and Singh, 2005; Mishra and Parida, 2006; Belkacem and Abderrahmane, 2008), but there is a gap in research about the effect of drain size on the stability of upstream slope in drawdown condition. In addition, the above-mentioned studies of the steady state focused either on determination of the appropriate drain length in a horizontal drain or the thickness of a toe drain. In this study, the goal is to take the parameter of thickness into account in a horizontal drain and consider the efficiency of the combination of length and thickness in both steady and transient conditions. Therefore, horizontal drains with various thicknesses and different lengths (ranging from the minimum to maximum effective lengths) are applied and their efficiencies are evaluated both in the steady and transient states in a laboratory model.

2. Steady state seepage in an embankment dam with a horizontal drain

Numerov (1942) performed research on the application of a drain in an embankment dam and presented a primary method to determine the location of the phreatic line in an embankment dam with a drainage system. Today, there are different types of drains that are applied to embankment dams such as chimney drain, toe drain, and horizontal drain. The chimney drain is usually utilized at the downstream side of the impermeable clay core in zoned embankment dams and the toe drain and horizontal drain have been widely applied to homogeneous embankment dams. In this study, the focus will be on the horizontal drain, which has been widely used in embankment dams of medium height, which are usually 20-60 m high. In the literature, embankments higher than 60 m and lower than 20 m are classified as the small and high embankment dams, respectively (USBR, 2003). The Vega Dam, constructed by USBR, which is 50 m high, is an example of the application

of horizontal drain system. In the last decade, some researchers suggested practical methods to determine the suitable length of horizontal drains (USBR, 2003; Chahar, 2004). Chahar (2004) presented relationships to determine the minimum and maximum effective drain lengths that can prevent the seepage flow from touching the downstream slope (Eqs. (1), (2), and (3)). The mentioned equations have been derived considering the distance of the phreatic line from the downstream sloping face, which is defined as the downstream slope cover (Figure 1), while the method presented by USBR (2003) did not take the downstream slope cover into account. This is the advantage of Chahar's equations in comparison with the method proposed by USBR (2003). Figure 1 illustrates the cross section of a homogeneous embankment dam and the parameters of Chahar's equations in isotropic condition.

$$d^*_{\max} = \frac{[F^*_B(m+n)+T^*]}{\sqrt{(1+n^2)}} \tag{1}$$

$$l^*_{\min} = \frac{1+n^2}{2n^2}\left\{0.3m+n+F^*_B(m+n)+T^* - \sqrt{[0.3m+n+F^*_B(m+n)+T^*]^2-n^2}\right\} \tag{2}$$

$$l^*_{\max} = F^*_B(m+n)+T^*+\frac{1+n^2}{2n^2}\left[0.3m+n-\sqrt{(0.3m+n)^2-n^2}\right] \tag{3}$$

where l and d are drain length and downstream slope cover, respectively. The asterisk represents the dimensionless form of the parameters denoted in Figure 1 by dividing each of them by h and this dimensionless presentation of results can be used to predict the behavior in prototype. Equations (1) and (3) determine the maximum downstream slope cover and the maximum effective length of the drain, respectively. In Eq. (2), the minimum length is derived so that the downstream slope cover is greater than the capillary rise above the phreatic line. Hence, the capillary front is unlikely to touch the downstream slope and piping is prevented. In this study, the method of Chahar (2004) is adopted to determine the minimum and maximum effective lengths of the horizontal drain and a combination of obtained lengths and different thicknesses is applied to a laboratory model of an embankment dam to evaluate the effect of drain size on the phreatic line.

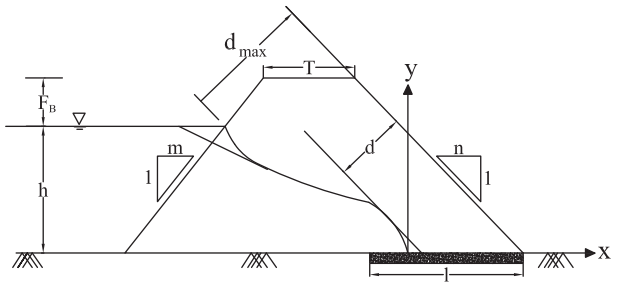

Figure 1. Geometric parameters and downstream slope cover (Chahar, 2004).

3. Transient seepage in rapid drawdown condition

Transient seepage in an embankment dam is defined as the temporal variation of seepage flow characteristics including pore water pressure and the location of the phreatic surface. As mentioned in the previous section, when the water level in the reservoir of an embankment dam falls, the hydrostatic pressure that nullifies the

destructive effect of pore pressure on the upstream slope is gradually or suddenly removed. Hence the upstream slope may become unstable and subject to collapse, which is the result of saturated pores and seepage flow towards the reservoir (Figure 2).

When the water level in a reservoir falls at such a quick rate that no change in pore pressure occurs at the upstream slope immediately after drawdown and the phreatic surface keeps its previous position, it is called rapid drawdown. The stability of the upstream slope in rapid drawdown condition mainly depends upon the rate and ratio of drawdown, the hydraulic conductivity of the material, and drainage. Lane and Griffiths (1997), Tran (2004), and Viratjandr and Michalowski (2006) presented similar results and concluded that the factor of safety (FS) for upstream slope stability decreased noticeably when the water level after drop was almost one-third of the embankment height. Tran (2004) performed a case study of rapid drawdown in the Dau Tieng Dam and considered the parameter of drawdown ratio (L/H) where H is the dam height and L is the water depth after drawdown (Figure 2). As shown in Figure 3, the FS value decreases approximately 34% at the drawdown level of H/3 and almost 43% at complete emptying. Therefore, the critical drop rate of the FS value occurs before the complete emptying of the reservoir, which imposes excessive pore pressure on the upstream slope.

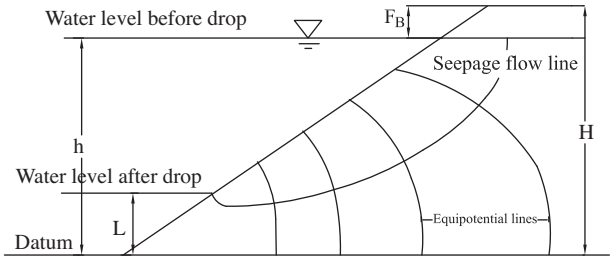

Figure 2. Seepage flow towards the upstream reservoir after water level drop (Kerkes and Fassett, 2006).

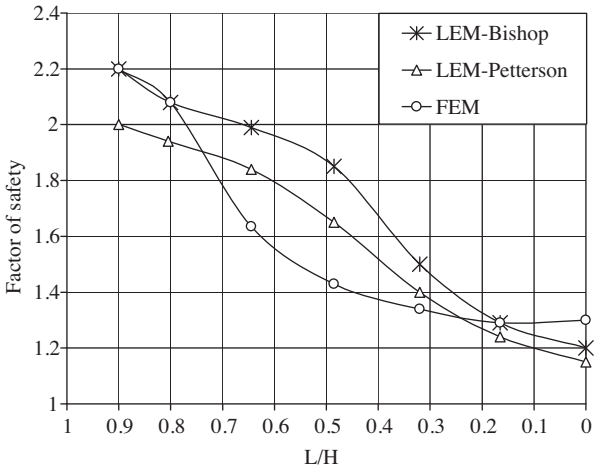

Figure 3. FS values for upstream slope stability in rapid drawdown (RDD) condition by different methods (Tran, 2004).

In this study, the Ordinary Method of Slices (OMS) (Anderson and Richards, 1987), which is simple to use in laboratory works and incorporates the effect of pore pressure, is adopted to analyze the stability of the upstream slope.

4. Experimental set-up

The physical model of an embankment dam was constructed in a Seepage and Drainage Tank as illustrated in Figure 4. It was equipped with 42 piezometers to measure the pore water pressure in steady state experiments. In addition, the pressure sensors were installed at 4 points (A, B, C, and D in Figure 5) on the upstream slope to accurately record the temporal variation of pore pressure in the case of rapid drawdown. Table 1 presents the properties of the homogeneous low permeable body material and the drain materials applied to build the

embankment dam. As presented in Table 2, the filter materials were selected based on Terzaghi's criterion (USACE, 1953) and also using the enhanced model of filter design presented in Indraratna and Raut (2006).

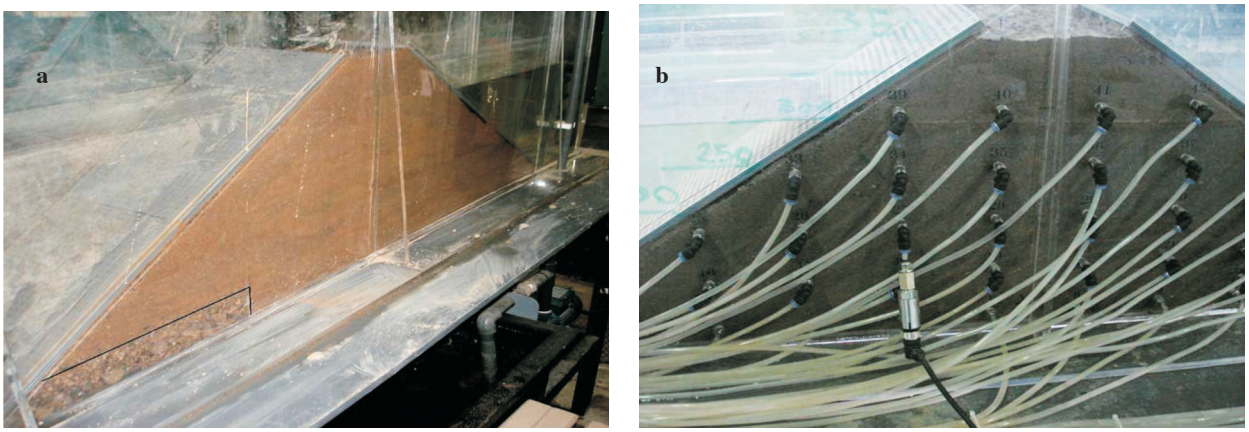

Figure 4. Experimental set up; (a) horizontal drain in the back view; (b) series of piezometers and a pressure sensor in front view.

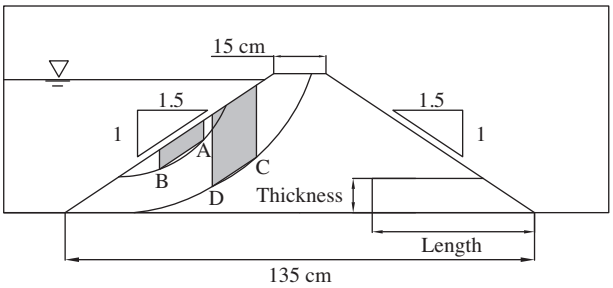

Figure 5. Schematic view of the position of sensors for recording the temporal variations of pore pressure.

Table 1. Properties of the embankment body soil and the drain material.

Soil type Unified classification	Optimum moisture of soil (Standard proctor) %	Plastic limit (PL) %	Liquid limit (LL) %	Soil hydraulic conductivity (cm/s)	Drain type Unified classification	Drain hydraulic conductivity (cm/s)
SP-SC	16	23.9	36.5	2.8×10^{-5}	GW	0.97

In Terzaghi's criterion 15% by mass of the filter materials and 85% by mass of the body materials are finer than the particle diameters denoted by $D_{15(\text{Filter})}$ and $D_{85(\text{Body material})}$, respectively. The parameters of the enhanced model are shown in Figure 6. Since well-graded materials were selected for the filter, H/F ratios were calculated for $F \leq 20$ (as proposed in Figure 6). The reader is referred to Indraratna and Raut (2006) for further details. According to Table 2, the minimum value of H/F is greater than unity. Therefore, the selected filter material satisfies the criterion of an enhanced model as well as Terzaghi's criterion. The particle size distributions of the body and filter materials are shown in Figure 7. The geometric scale of 1:50 was selected in physical modeling and considering the minimum height of 20 m for a medium embankment dam, the physical model was built in the Seepage and Drainage Tank. Table 3 presents the geometric parameters of the physical

model. In order to establish a homogeneous compacted embankment, the dried sieved materials were completely mixed together to make an almost homogeneous compound, which was then compacted in 3 layers with the optimum moisture value (presented in Table 1). In this research, there were some limitations associated with the scale effect on the particle size of embankment materials. For instance, if the appropriate particle size for embankment dam is scaled down according to the geometric scale, it falls within the range of very impermeable clays. Consequently, the capillary rise is not controlled within the small size of the embankment model and the effect of the drain on the downstream slope cover is not evaluated as desired. Therefore, a soil with a low percentage of clay was chosen to cope with the capillary rise. Another limitation was associated with the small width of the embankment that led to a 2D nature of seepage flow in laboratory experiments; it is naturally 3D in the prototype. Since the tail water depth imposes a hydrostatic pressure on lower parts of the downstream slope and has a stabilizing effect on it, in this research the tail water depth was set to zero. Hence, the entire downstream slope was subject to piping and the efficiency of drains could be better understood. Equations (2) and (3) were used to determine the minimum and maximum drain lengths of the physical model. In addition, another drain length was selected in the range of the minimum and maximum lengths and referred to as the medium length. Mishra and Parida (2006) suggested that the maximum effective height (thickness) of the toe drain is about one-third of the embankment height but there is still a gap in research about the effect of thickness on the efficiency of the horizontal drain. In this study, 3 different thicknesses (referred to as the minimum, medium, and maximum thickness) were selected and applied in combination with the mentioned drain lengths. Table 4 presents all the lengths and thicknesses of the horizontal drain that were applied to the physical model. During the tests, the maximum water depth in the reservoir (refer to Table 3) was used and the effect of horizontal drain size in lowering the phreatic line was tested in steady seepage condition. Then the horizontal drain size was tested under the rapid drawdown condition. Since the upstream slope is the most sensitive part of the embankment dam during rapid drawdown, 4 sensors were installed on 2 slices at the upstream slope (AB and CD in Figure 5) to record the variations in pore pressure. As a result of the small size of the model and the low percentage of clay in fine grained material, the effect of stress and strain, i.e. consolidation after drawdown, was ignored. Some initial tests were accomplished prior to the experiments on the physical model without using drains and the slip surfaces (of Figure 5) were observed applying the smallest and largest drawdown ratios. In fact, AB and CD were 2 slices on 2 observed slip surfaces during the preliminary tests (without application of the drain). After the application of drawdown ratios, the effect of drain size on the factor of safety was studied on AB and CD. Meanwhile, it is not claimed that the observed slip surfaces are the only possible ones in rapid drawdown condition but the goal of this paper is only to consider the effect of drain size on the stability of some points of the embankment dam model that were subject to collapse (when no drain was used). Finally, different drawdown ratios were applied and the temporal variations in pore pressure were recorded by the pressure sensors. The factor of safety for each drain size is presented in the following section.

Table 2. Evaluation of the efficiency of filter materials.

Method	Effective filter	Ineffective research	Current research filter	Status of applied
Terzaghi (USACE, 1953)	$\frac{D_{15(Filter)}}{D_{85(Body\,material)}} \leq 5$	$\frac{D_{15(Filter)}}{D_{85(Body\,material)}} > 5$	$\frac{D_{15(Filter)}}{D_{85(Body\,material)}} = 2.86$	Efficient
Indraratna and Raut (2006)	$\frac{H}{F} \geq 1$	$\frac{H}{F} < 1$	$(\frac{H}{F})_{\min} = 1.05$	Efficient

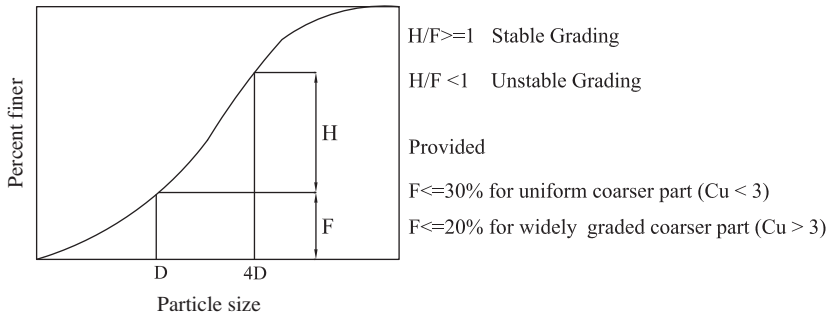

Figure 6. Graphical assessment of the stability of filters (Indraratna and Raut, 2006).

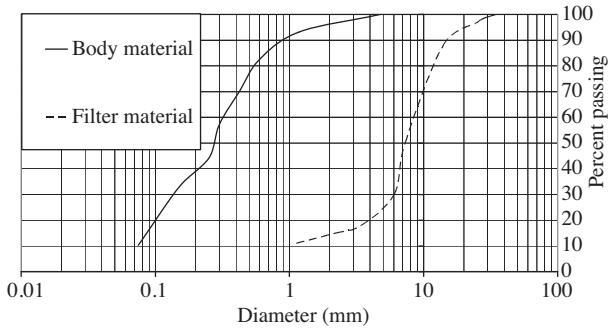

Figure 7. Particle size distributions of the materials of embankment body and filter.

Table 3. Geometric parameters of the physical model of embankment dam.

Downstream slope (v:h)	Upstream slope (v:h)	Crest width (cm)	Height of embankment (cm)	Maximum depth in reservoir (cm)
1:1.5	1:1.5	15	40	35

Table 4. Different lengths and thicknesses of the horizontal drain.

Minimum length (cm)	Medium length (cm)	Maximum length (cm)	Minimum thickness (cm)	Medium thickness (cm)	Maximum thickness (cm)
15	25	38	2.5	6	9.5

5. Results and discussion

5.1. Experiments of the steady state

In this section, the results of experiments with the application of different drain sizes are presented in the form of phreatic surfaces and d*-l* graphs. It can give good information to the reader about the simultaneous effect of drain length and thickness in steady state experiments. The tests for each drain size were carried out and the downstream slope cover was measured for all of the observed phreatic surfaces. Figure 8 illustrates the phreatic lines for the minimum length and the applied thicknesses. It is obvious that none of the phreatic lines was controlled well within the embankment body. Thus for the minimum thickness the phreatic line touched the downstream slope and the slope cover was zero somewhere close to the toe. For the medium and maximum drain thicknesses, none of the phreatic lines touched the downstream slope but they were very close to the slope.

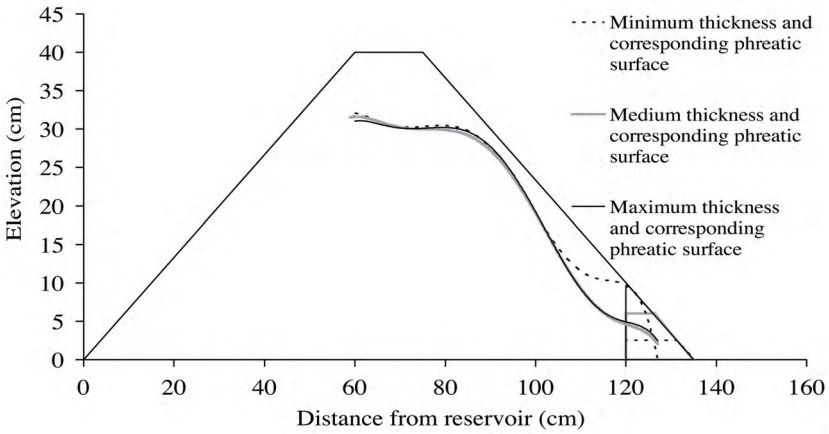

Figure 8. Observed phreatic lines for the minimum drain length.

Figure 9 shows the phreatic lines obtained for the medium drain length. It is observed that all the phreatic lines were controlled well within the embankment and none of them intersected the downstream slope. Comparing the phreatic lines in Figures 8 and 9, it is evident that the increased length caused a larger slope cover but the increased thickness had less effect on the slope cover, especially in the case of minimum drain length.

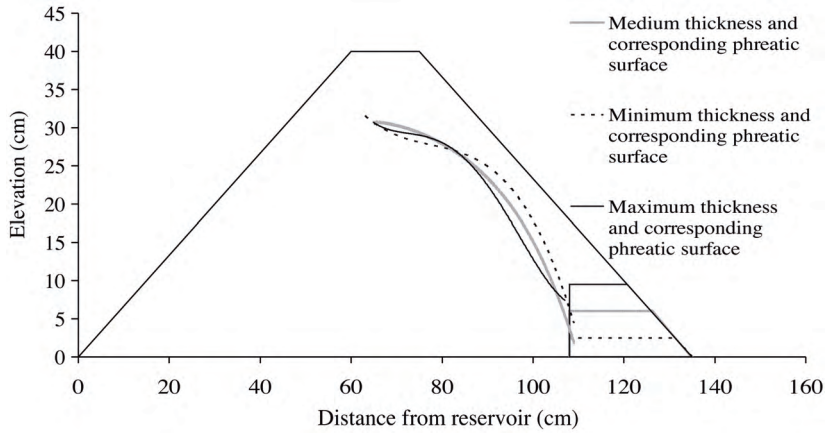

Figure 9. Observed phreatic lines for the medium drain length.

Figure 10 demonstrates the phreatic lines of the maximum drain length. It is indicated that for the minimum thickness the phreatic line was confined well within the embankment dam but the slope cover was similar to that of the medium length. In addition, the downstream slope cover increased dramatically for the medium and maximum thicknesses. This highlights the positive effect of drain thickness on lowering the phreatic line, especially when a drain with maximum effective length is employed. It is concluded from Figures 8, 9, and 10 that when the drain length was closer to the maximum effective value obtained from Eq. (3) the greatest slope covers were observed for the medium and maximum applied thicknesses. On the other hand, if the drain length selected is close to the value of minimum effective length, the increased thickness has a negligible effect on improving the slope cover.

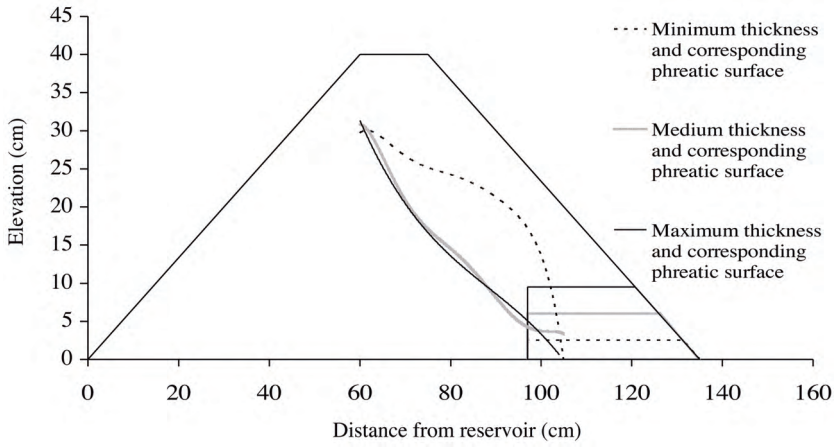

Figure 10. Observed phreatic lines for the maximum drain length.

Chahar (2004) presented several graphs to explain the relationship between l* and d* without taking the drain thickness into account. In Figure 11 the lines fitted to the data obtained in this study (considering the drain thickness) are displayed and compared with that given by Chahar (2004). All of the experimental data are located below Chahar's line and the line related to the minimum thickness has almost the same inclination as the Chahar's but with a different intercept. It demonstrates that even the minimum applied thickness has a positive effect on increasing the downstream slope cover and results in a greater downstream slope cover than the conventional horizontal drain (with negligible thickness). As the thickness increased, lines with milder slopes were obtained and greater downstream slope covers were achieved for lower drain lengths. Comparing the graphs of medium and maximum thickness, it is observed that the corresponding lines are almost parallel and close to each other. Comparing with the results of medium thickness (6 cm) it is observed that when the maximum thickness value of this research (9.5 cm) was applied a little improvement in downstream slope cover was achieved. Meanwhile, the inclinations of d*-l* graphs for the medium and maximum thickness are almost the same.

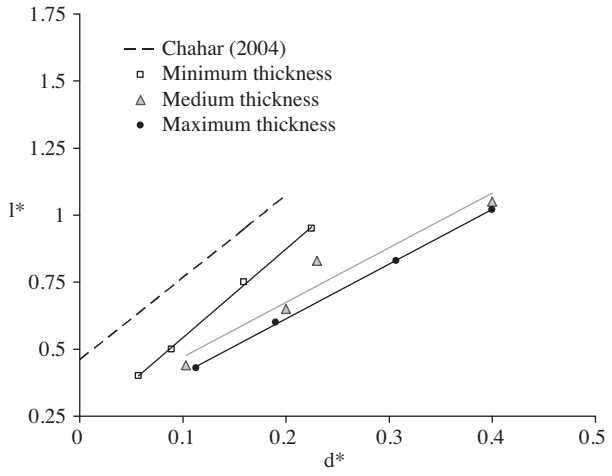

Figure 11. Downstream slope cover against the drain length for different thicknesses applied in this study compared with Chahar's result.

5.2. Factor of safety in rapid drawdown condition

In this section, the results of experiments for the rapid drawdown condition are presented and the effect of horizontal drain size on the stability of upstream slope is analyzed. In this regard, multiple graphs are provided that display the FS value against drawdown ratio and time. The drawdown ratio in the presented graphs is defined as L_d/h where $L_d = h-L$ (based on the parameters shown in Figure 2) and applying different drawdown ratios the FS values were calculated after drawdown on AB and CD. Figure 12 shows the factor of safety on AB against the drawdown ratio for all combinations of length and thickness. It is observed that with increase in drawdown ratio the FS graphs demonstrate the descending trend for the minimum drain length and all of the thicknesses. The reduction in FS values is due to the excess pore pressure after drawdown and indicates the prevailing undrained behavior on AB for the minimum drain length. In this paper, the expression "undrained behavior" represents the reduction of the factor of safety after an applied drawdown ratio and indicates that the applied drain size is unable to dissipate the excessive pore pressure immediately after drawdown, which leads to the decrease in the FS value. On the other hand, the "drained behavior" occurs when the drains are able to dissipate the pore pressure immediately after drawdown and this causes the increase in FS values.

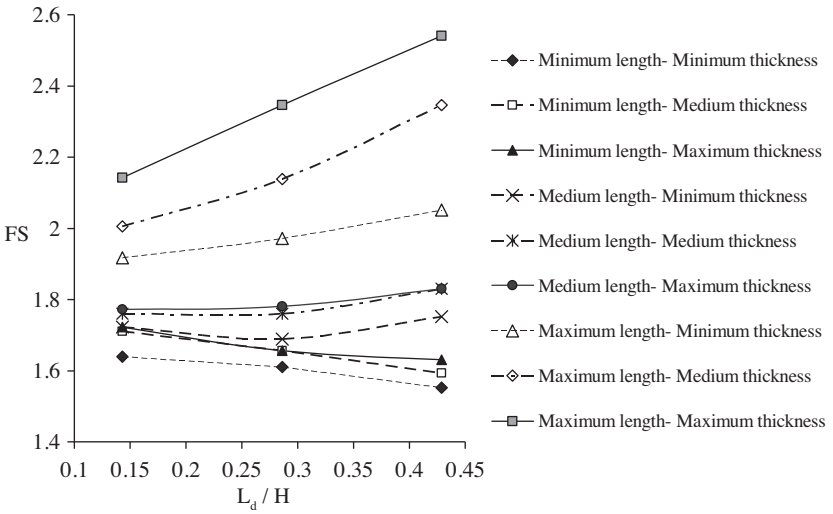

Figure 12. Factor of safety (FS) against drawdown ratio on AB.

For the medium drain length and minimum thickness, the reduction in FS values was perceived after the beginning of drawdown. When higher drawdown ratios and greater thicknesses were applied the descending trend of FS curves turned into a slightly ascending trend, which indicates the gradual emerging of drained behavior on AB. Therefore, as the time elapsed after the beginning of drawdown and higher drawdown ratios were applied, the drain with medium length was able to nullify the excess pore pressure and created the drained behavior.

For the maximum effective length, the ascending trend of the curves demonstrates the drained behavior. However, the curves related to the medium and maximum thicknesses are steeper than that of the minimum thickness, which indicates the noticeable effect of thickness on creating greater drained behaviors and increasing the FS value. Therefore, it shows the positive effect of thickness on the stability of the embankment dam in rapid drawdown condition, especially for the maximum effective length. It is somehow similar to the results taken from the steady state analysis where the efficiency of thickness in lowering the phreatic surface was noticeable for higher drain lengths.

Figure 13 presents the FS values on CD for the same drain sizes and drawdown ratios as in Figure 12. The curves related to the minimum effective length are close to each other and follow a mild ascending trend. They represent a slightly drained behavior and the small space between them indicates the negligible effect of thickness on increasing the factor of safety on CD. According to Figure 13, the inclination and the distance between FS curves increase when longer drains are applied but the curves have slightly less steepness than the similar curves in Figure 12. A comparison between the FS values on AB and CD gives interesting results. For example, Figure 13 illustrates the slightly drained behavior for the minimum length on CD, whereas the application of the same drain size leads to the undrained behavior and the descending trend of the FS values on AB (Figure 12). This difference results from the fact that when no drain or the minimum drain length is applied the prevailing direction of seepage flow after drawdown is towards the reservoir, which causes the decline in FS values on AB (which is closer to the upstream sloping face). For the medium length and minimum thickness when the drawdown ratio reached the values of greater than 0.3, the undrained behavior on AB changed to a drained behavior, but for the medium length and the medium thickness the undrained behavior was observed from the beginning of drawdown. Consequently, the dominant seepage flow direction turned back towards the drain and AB became more stable. In such a case, the pore pressure in the vicinity of the upstream slope declined dramatically and the obtained FS value on AB was greater than CD. According to the results the FS values varied in the range of 1.55-2.54 and 1.28-2.22 on AB and CD, respectively. Meanwhile, the ultimate FS value on AB is greater than CD for a given drain size. These experiments prove the significant role of drain size in increasing the slope stability, especially in the vicinity of the upstream sloping face. Generally, the application of a drain with the maximum effective length led to the absolutely drained behavior on both AB and CD and increased the stability of the upstream slope. At the next step, drains with the maximum length were tested to analyze the temporal variation of FS in drained condition. In this regard, the pore pressure was recorded on AB and CD for the minimum and maximum thicknesses to determine the effect of increased thickness on temporal variations of the FS value after drawdown.

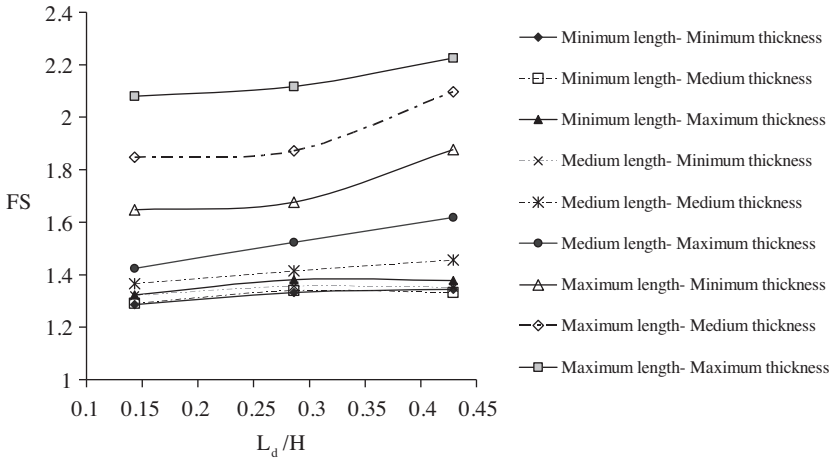

Figure 13. Factor of safety (FS) against drawdown ratio on CD.

Figure 14 illustrates the temporal variations of the FS value on AB and CD based on the variation of pore pressure after drawdown. Figure 14-a shows that for the maximum effective length and the minimum thickness the initial FS value after drawdown on CD is greater than AB. It can be attributed to the initial influence of drain on CD, which is closer to the drain. As the time elapses since the outset of rapid drawdown and the drain affects the upstream slope, the direction of seepage flow changes from upstream (Figure 2) towards

the drain and it makes the surface area of the upstream slope (slice AB) completely safe against sliding. It is observed that the temporal variation of the FS value on AB is greater than on CD. It can be attributed to quicker removal of pore pressure on AB than CD at the moment that the drain completely affects the upstream slope. Figure 14-b presents the temporal variation of the FS value on AB and CD for the maximum drain length and the maximum thickness. As shown in Figure 14-b, for the maximum thickness the initial values of FS on both AB and CD are greater than those for the minimum thickness. A comparison between Figures 14-a and 14-b indicates that as the drain thickness increases to the maximum value the initial increase in FS value for CD is greater than for AB due to the closer location of CD to the drain. However, an equal or slightly greater factor of safety is achieved for AB as the time elapses and the drain affects the superficial areas of the upstream slope. The curves in Figure 14-b coincide as the time elapses after the beginning of drawdown and it is in contrast with the trend of curves in Figure 14-a. It represents the capability of the drain with maximum thickness to make a quicker reaction to rapid drawdown than the drain with minimum thickness. Thus it can uniformly nullify the pore pressure and create the same FS in the entire upstream slope (on both AB and CD). On the slice AB, the ultimate FS values obtained from the minimum and maximum thicknesses were 2.6 and 2.7, respectively. Finally, on CD, the ultimate FS values for the minimum and maximum thicknesses were 2.3 and 2.7, respectively.

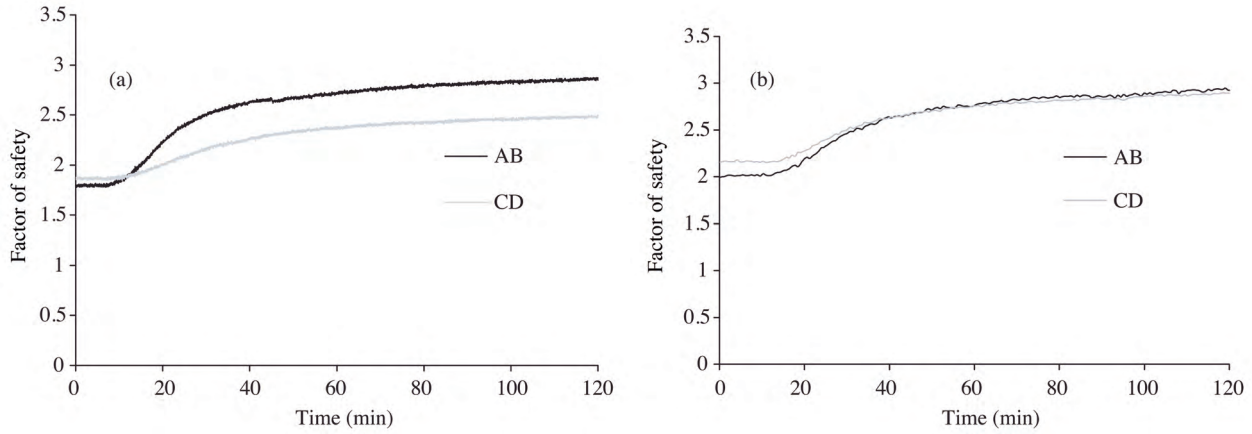

Figure 14. Temporal variation of FS in drained condition; (a) for maximum length and minimum thickness; (b) for maximum length and maximum thickness.

6. Conclusion

In steady state experiments, the lines fitted to the experimental data (d*-l* graphs) were located below the results of Chahar (2004). Therefore, greater downstream slope covers were obtained during the tests even for the minimum thickness. d* for the thickness of 2.5 cm varied in the range of 0.057-0.225, while for the thicknesses of 6 and 9.5 cm it varied within greater ranges (0.103-0.4 and 0.112-0.41, respectively). In other words, greater slope covers were obtained with the application of lower drain lengths. As mentioned above, the maximum d* value was 0.41, which is almost twice the d* value obtained for the minimum thickness and 2.5 times Chahar's result. Moreover, the increase in thickness from 6 cm to 9.5 cm had a negligible effect on d* values. In transient state after drawdown, the factor of safety on AB and CD varied in the ranges of 1.55-2.54 and 1.28-2.22, respectively. The application of the 15 cm long drain and all of the thicknesses led to

the undrained behavior on AB and a slightly drained behavior on CD. The drain size of 25 cm long and 2.5 cm thick showed the drained behavior for $L_d/h > 0.3$. The medium length for thicknesses of 6 and 9.5 cm and the length of 38 cm for all of the thicknesses demonstrated the drained behavior. Moreover, the factor of safety for the thickness of 2.5 cm after almost 40 min from the beginning of drawdown was 2.25 and 2.6 on AB and CD, respectively. Finally, the factor of safety for the drain of 9.5 cm thick was 2.7 on both AB and CD. This shows that the increased thickness could establish a uniform stability on AB and CD, whereas for the thickness of 2.5 cm or no thickness, as assumed in Chahar (2004), a higher factor of safety is expected on AB, which demonstrates higher stability against superficial slip surfaces.

Nomenclature

d^*_{max}	maximum dimensionless downstream slope cover
l^*_{min}	minimum dimensionless effective length of drain
l^*_{max}	maximum dimensionless effective length of drain
F^*_B	dimensionless free board
T^*	dimensionless top (crest) width of embankment
FS	factor of safety

References

Anderson, M.G. and Richards, K.S., "Slope Stability: Geotechnical Engineering and Geomorphology", John Wiley and Sons, N.Y, 1987.

Baker, R., Rydman, S. and Talesnick, M., "Slope Stability Analysis for Undrained Loading Conditions", Intl. Jr. Num. and Anal. Methods Geomech., 17, 14-43, 1993.

Belkacem, M. and Abderrahmane B., "A Design Chart for Positioning a Drainage Blanket in an Earth Dam", EJGE, Technical Note, Vol. 13, Bund. D, 2008.

Berilgen, M.M., "Investigation of Stability of Slopes under Drawdown Conditions", J. Computers and Geotech., 34, 81-91, 2007.

Chahar, B.R., "Determination of Length of Horizontal Drain in Homogeneous Earth Dams", ASCE, Jr. Irrigation & Drainage Eng., No. 6, November/December, 130, 530-536, 2004.

Duncan, J.M. and Wright, S.G., "Soil Strength and Slope Stability", Hobken (NJ): John Wiley & Sons, 2005.

Fell, R., Wan, C.F., Cyganiewicz, J. and Foster, M., "Time for Development of Internal Erosion and Piping in Embankment Dams", Jr. Geotech. Geoenviron. Eng., 129, 307-314, 2003.

Foster, M., Fell, R. and Spannagle, M., "The Statistics of Embankment Dam Failures and Accidents", Can. Geotech. Jr., 37, 1000-1024, 2000.

Indraratna, B. and Raut, A.K., "Enhanced Criterion for Base Soil Retention in Embankment Dam Filters", Jr. Geotech. Geoenviron. Eng., ASCE, 132, 1621-1627, 2006.

Kerkes, D.J. and Fassett, J.B., "Rapid Drawdown in Drainage Channels with Earthen Side Slopes", In Proceedings of the ASCE Texas Section Spring Meeting, Beaumont, TX, 19-22 April, 2006.

Lane, P.A. and Griffiths, D.V., "Assessment of Stability of Slopes under Drawdown Conditions", Jr. Geotech. and Geoenv. Eng., 126, 443-450, 2000.

Lane, P.A. and Griffiths, D.V., "Finite Element Slope Stability Analysis", In Proceedings of the 6th Intl. Symposium on Numerical Models in Geomech. (NUMOG VI) Montreal Que., 2-4 July, A.A. Balkema, Rotterdam, Netherlands, 589-593, 1997.

Lowe, J. and Karafiath, L., "Effect of Anisotropic Consolidation on the Undrained Shear Strength of Compacted Clays", Proc. Research Conf. on Shear Strength of Cohesive Soils, Boulder, 237-258, 1980.

Mattsson, H., Hellström, J.G.I. and Lundström, T.S., "On Internal Erosion in Embankment Dams: A Literature Survey of the Phenomenon and the Prospect to Model It Numerically", Research Report, Luleå University of Technology, 2008.

Mishra, G.C. and Parida, B.P., "Earth Dam with Toe Drain on an Impervious Base", ASCE, Intl. Jr. Geomechanics, November/September, 379-388, 2006.

Mishra, G.C. and Singh, A.K., "Seepage through a Levee", ASCE, Intl. Jr. Geomechanics, March, 74-79, 2005.

Numerov, S.N., "Solution of Problem of Seepage without Surface of Seepage and without Evaporation or Infiltration of Water from Free Surface", P M M, 6, 1942.

Svano, G. and Nordal, S., "Undrained Effective Stability Analysis", Proc. of the Ninth European Conf. on Soil Mech. and Found. Eng., Dublin, 1987.

Tran, T.X., "Stability Problems of an Earthfill Dam in Rapid Drawdown Condition", Doctoral Dissertation, Slovak University of Technology, Bratislava, Slovak Republic, 2004.

US Army Corps of Engineers (USACE), "Engineering and Design Manual of Slope Stability", Engineer Manual EM 1110-2-1902, Department of the Army, Corps. of Engineers, Washington (DC), 2003.

United States Army Corps of Engineers (USACE), "Investigation of Filter Requirements for Underdrains", U.S. Waterways Experiment Station, Vicksburg, Miss., Tech. Memo. No. 3–360, 1953.

United States Bureau of Reclamation (USBR), "Design of Small Dams", Oxford & IBH, New Delhi, 2003.

Viratjandr, C. and Michalowski, R.L., "Limit Analysis of Submerged Slopes Subjected to Water Drawdown", Can. Geotech. Jr., 43, 802-814, 2006.

Wright, S.G. and Duncan, J.M., "An Examination of Slope Stability Computation Procedures for Sudden Drawdown", Report GL-87-25, US Army Corps Engineering, Waterway Experiment Station Vicksburg (MS), 1987.